Proton Nuclear Magnetic Resonance Investigation of the [2Fe-2S]$^{1-}$-Containing "Rieske-Type" Protein from *Xanthobacter* Strain Py2[†]

Richard C. Holz,* Frederick J. Small,[§] and Scott A. Ensign*

Department of Chemistry and Biochemistry, Utah State University, Logan, Utah 84322

Received July 28, 1997; Revised Manuscript Received September 19, 1997[⊗]

ABSTRACT: Proton NMR spectra of the Rieske-type ferredoxin from *Xanthobacter* strain Py2 were recorded in both H_2O and D_2O buffered solutions at pH 7.2. Several well-resolved hyperfine-shifted ^{1}H NMR signals were observed in the 90 to −20 ppm chemical shift range. Comparison of spectra recorded in H_2O and D_2O buffered solutions indicated that the signals at −11.4 (L) and −15.5 (M) ppm were solvent-exchangeable and thus were assigned to the two histidine N$^{\epsilon 2}$H protons. The remaining observed signals were assigned based upon chemical shift, T_1 values, and one-dimensional nuclear Overhauser effect (nOe) saturation transfer experiments to either C$^{\beta}$H or C$^{\alpha}$H protons of cluster cysteinyl or histidine ligands. Upon oxidation of the [2Fe-2S] cluster, only two broad resonances were observed, indicating that the two Fe(III) ions are strongly antiferromagnetically coupled. In addition, the temperature dependence of each observed hyperfine-shifted signal in the reduced state was determined, providing information about the magnetic properties of the [2Fe-2S]$^{1-}$ cluster. Fits of the temperature data observed for each resonance to equations describing the hyperfine shift with their Boltzmann weighting factors provided a ΔE_L value of 185 ± 26 cm^{-1} which, in turn, gives $-2J$ as 124 cm^{-1}. These data indicate that the two iron centers in the reduced [2Fe-2S] Rieske-type center are moderately antiferromagnetically coupled. The combination of these data with the available spectroscopic and crystallographic results for Rieske-type proteins has provided new insights into the role of the Rieske-type protein from *Xanthobacter* strain Py2 in alkene oxidation.

Proteins containing Rieske-type [2Fe-2S] clusters play important roles in many biological electron transfer reactions. For example, Rieske-type clusters are components of mitochondrial, chloroplastic, and bacterial respiratory chain complexes (*1*−*7*). Rieske-type iron−sulfur proteins have also been found to serve as electron transfer components of a broad group of bacterial dioxygenases that catalyze the NADH- and O_2-dependent oxidation of aromatic compounds (*8*−*12*), as well as two recently characterized monooxygenases: toluene-4-monooxygenase from *Pseudomonas mendocina* (*6*) and alkene monooxygenase from *Xanthobacter* strain Py2 (*13*). Iron−sulfur proteins with Rieske-type centers have also been identified in organisms as diverse as the archaebacteria, although no definitive functions have yet been assigned for these particular proteins (*1*, *4*).

Rieske-type [2Fe-2S] clusters differ from the classical plant-type [2Fe-2S] clusters in the nature of the amino acid ligands that coordinate the diiron center. While plant-type [2Fe-2S] clusters are ligated solely by cysteine residues, Rieske-type [2Fe-2S] clusters have mixed coordination: one iron atom is ligated to two cysteine residues, while the other iron atom is ligated to the δ-nitrogen atoms of two histidine residues (*14*). This novel noncysteine ligation apparently contributes to the higher reduction potentials of proteins containing Rieske-type centers and provides spectroscopic signatures that allow these two classes of proteins to be easily differentiated (*3*, *6*, *14*−*16*).

While the [2Fe-2S] clusters of Rieske-type iron−sulfur proteins have been extensively characterized by electronic spectroscopy [*e.g.*, UV/visible, EPR,[1] circular dichroism, and ENDOR (*3*, *6*, *14*−*16*)], there is little NMR information available on this class of proteins. ^{1}H NMR spectroscopy is a very sensitive method with which to study paramagnetic metal cluster-containing proteins (*17*−*23*). Only protons proximate to the metal cluster are shifted out of the diamagnetic envelope, providing a fingerprint of the metal ligand environment. In addition, a wealth of magnetic information on spin-coupled systems (*e.g.*, 4Fe-4S clusters) can be obtained by measuring the temperature dependence of the hyperfine-shifted signals (*17*, *18*, *21*, *22*). These studies allow local spin magnetization to be characterized without interference from the bulk susceptibility. Ferredoxin-type proteins that contain [2Fe-2S] clusters have been intensely studied by ^{1}H NMR methods and a great deal of information about the cluster environment as well as the electronic properties of the cluster has been obtained (*17*, *18*, *21*, *22*).

To date, only a single ^{1}H NMR spectrum of a Rieske-type protein has been reported (*23*). This study revealed several hyperfine-shifted protons in the 40 to −5 ppm chemical shift range; however, no signal assignments were provided. In an effort to gain further insight into the structural and magnetic properties of Rieske-type [2Fe-2S]$^{1-}$

[†] This work was supported by the National Science Foundation (CHE-9422098, R.C.H.) and the National Institutes of Health (GM-51805, S.A.E.). The Bruker ARX-400 NMR spectrometer was purchased with funds provided by the National Science Foundation (CHE-9311730) and Utah State University.

* Address correspondence to this author: Phone (801) 797-2609; Fax (801) 797-3390; e-mail rholz@cc.usu.edu.

[§] This paper is dedicated in memory of Frederick Joseph Small, a Ph.D. candidate and Thomas F. Emery Scholar who died in a tragic accident on July 15, 1997.

[⊗] Abstract published in *Advance ACS Abstracts,* November 1, 1997.

[1] Abbreviations: ^{1}H NMR, proton nuclear magnetic resonance; EPR, electron paramagnetic resonance; ENDOR, external nuclear double resonance; Tris, tris(hydroxymethyl)aminomethane; nOe, nuclear Overhauser effect; Mops, 3-(*N*-morpholino)propanesulfonic acid.

S0006-2960(97)01831-X CCC: $14.00

proteins, we have recorded ^{1}H NMR spectra of the Rieske-type ferredoxin from *Xanthobacter* strain Py2 in both the reduced and oxidized states. Analysis of the hyperfine-shifted signals in H_2O and D_2O buffered solutions, T_1 values, and nuclear Overhauser effect (nOe) difference spectra have allowed, for the first time, the complete assignment of the hyperfine-shifted ^{1}H NMR resonances of a $[2Fe\text{-}2S]^{1-}$ Rieske-type cluster. The temperature dependence of each hyperfine-shifted signal was determined, which provides information about the magnetic properties of the $[2Fe\text{-}2S]^{1-}$ cluster. The combination of these data with the available spectroscopic and crystallographic results for Rieske-type proteins has provided new insights into the role of the Rieske-type protein from *Xanthobacter* strain Py2 in alkene oxidation.

MATERIALS AND METHODS

Purification of the Rieske-Type Ferredoxin and Preparation of NMR Samples. The Rieske-type ferredoxin was purified from cell-free extracts of *Xanthobacter* strain Py2 grown with propylene as the source of carbon as described previously (*13*). Protein samples for NMR were prepared in an argon-filled glove box with an oxygen concentration less than 1 ppm. Protein samples were prepared in 50 mM MOPS- (pH 7.2) buffered H_2O and D_2O solutions by passage through a Sephadex G-25 column (1.5 × 10 cm). Unless otherwise noted, the MOPS-buffered solutions were passed through a Chelex-100 column to remove trace metals prior to equilibration of the Sephadex column. Samples were concentrated to 1 mM in protein (2 mM in $[2Fe\text{-}2S]^{1-}$ cluster) by microfiltration with a Microcon-30 concentrator (Amicon, Beverly, MA). In all cases, sealed glass (5 mm) NMR tubes (Wilmad, Buena, NJ) were used to maintain an anaerobic environment.

Physical Methods. Proton NMR spectra were recorded on a Bruker ARX-400 spectrometer at 400.13 MHz. A presaturation pulse or a modified-DEFT multipulse sequence was used to suppress the water signal and the resonances in the diamagnetic region (*24*). The pulse sequence repetition rate was typically 3 s^{-1} with a spectral window of 83 kHz. Chemical shifts (in parts per million) were referenced to the residual water peak at 4.7 ppm. The ^{1}H NMR data were Fourier-transformed with an exponential apodization function as well as the application of a 30 Hz line broadening. Longitudinal relaxation times (T_1) were measured by the use of an inversion−recovery pulse sequence (180°−τ−90°). Plots of ln ($I_0 - I_\tau$) vs τ for each signal provided a straight line over all τ values investigated. Peak areas were determined as relative areas based on the 1:1 area ratio of signals A−D. Non-baseline-subtracted spectra were used to determine these areas by the cut and weigh method. Nuclear Overhauser effect (nOe) difference spectra were obtained at 300 K by computer manipulation of the free induction decay with the saturation pulse set alternatively on the signal of interest and a reference position for 10 ms. The pulse sequence repetition rate was typically 3 s^{-1} with a spectral window of 83 kHz. Steady-state nOe (η_{ij}) on signal i when signal j is saturated for a period of time t is given by

$$\eta_{ij} = \sigma_{ij}/\rho_i = 0.1\gamma^4 h^2 r_{ij}^{-6} \tau_c T_1 \qquad (1)$$

where σ_{ij} is the cross-relaxation between i and j, τ_c is the rotational correlation time of the molecule, ρ_i (T_1) is the spin−lattice relaxation rate of proton i, and r_{ij} is the distance between nuclei i and j. The remaining constants have their usual meaning. All nOe spectra were baseline-subtracted with either a cubic spline or fifth-order polynomial function to alleviate a sigmoidal baseline roll; therefore, nOe intensities shown in Figures 2 and 3 are not a quantitative measure of the percent nOe.

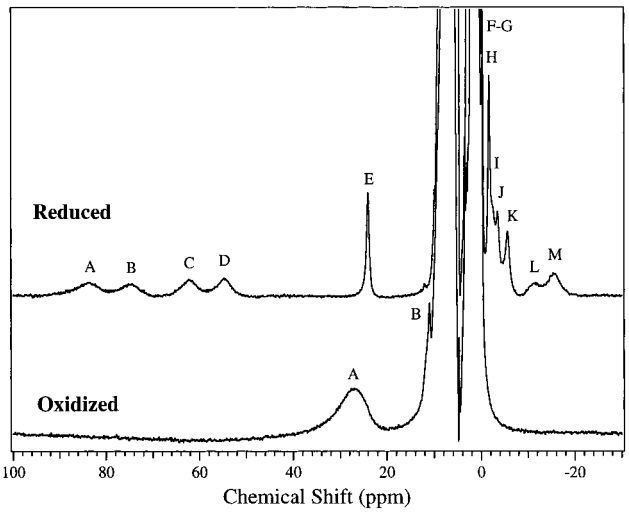

FIGURE 1: ^{1}H NMR spectra of (A) 1 mM sample of $[2Fe\text{-}2S]^{1-}$ (reduced) in H_2O at 300 K in 100 mM MOPS buffer and 200 mM NaCl, pH 7.0, and (B) 1 mM sample of $[2Fe\text{-}2S]^0$ (oxidized) in D_2O at 300 K in 100 mM MOPS buffer and 200 mM NaCl, pH 7.0.

Table 1: Properties of the Observed Hyperfine-Shifted ^{1}H NMR Resonances of the $[2Fe\text{-}2S]^{1+}$ Rieske-Type Ferredoxin from *Xanthobacter* Strain Py2

signal	assignment	chemical shift[a] (ppm)	line width[b] (Hz)	relative area[c]	T_1[d] (ms)	temperature dependence
A	Cys_A $C^\beta H$	82	1630	1	2	Curie
B	Cys_A $C^\beta H$	73	1550	1	2	Curie
C	Cys_B $C^\beta H$	62	1350	1	2	Curie
D	Cys_B $C^\beta H$	54	1200	1	3	Curie
E	Cys_B $C^\alpha H$	23.9	430	1	4	Curie
F	His_B $C^\alpha H$	−0.1	∼100	ND[e]	ND	ND[f]
G	His_B $C^\beta H$	−0.3	ND	ND	ND	ND[f]
H	His_A $C^\alpha H$	−1.4	230	ND	4	pseudo-Curie
I	His_B $C^\beta H$	−2.4	ND	1	4	pseudo-Curie
J	His_A $C^\beta H$	−3.2	230	1	3	pseudo-Curie
K	His_A $C^\beta H$	−5.4	380	1	3	pseudo-Curie
L[f]	His $N^{\epsilon 2}H$	−11.4	900	1	ND	ND
M[f]	His $N^{\epsilon 2}H$	−15.5	950	1	ND	pseudo-Curie

[a] All chemical shifts are in parts per million relative to the residual solvent signal at 4.7 ppm for H_2O. [b] Full width at half maximum. [c] Relative areas are based on the area of signals A−D. [d] T_1 values were obtained at 400 MHz and 25 °C. [e] ND, not determined. [f] Solvent-exchangeable.

RESULTS

^{1}H NMR Spectra of the Reduced and Oxidized Rieske-Type Protein from Xanthobacter Strain Py2. The 400 MHz ^{1}H NMR spectrum of the reduced Rieske-type protein in MOPS-buffered H_2O solution, pH 7.2, at 300 K is shown in Figure 1A. Thirteen hyperfine-shifted signals were observed in the 90 to −20 ppm chemical shift range (Table 1). hyperfine-shifted protons in the 100−10 ppm chemical shift range observed for proteins containing $[2Fe\text{-}2S]^{1-}$ clusters have previously been assigned to $C^\beta H$ and $C^\alpha H$ protons of

the cluster cysteinyl ligands (*17*, *21*, *22*). Based on chemical shifts and T_1 ($\propto r^6_{Fe-H}$) values, signals A (82 ppm; 2 ms), B (73 ppm; 2 ms), C (62 ppm; 2 ms), and D (54 ppm; 3 ms) were tentatively assigned to C$^\beta$H protons of cysteinyl ligands, while signal E (24 ppm; 4 ms) was tentatively assigned to a cysteinyl C$^\alpha$H proton. The relative areas of these signals indicated that each constituted approximately one proton. The two cysteine ligands bound to the [2Fe-2S] cluster would have a total of four C$^\beta$H and two C$^\alpha$H protons, so our initial assignments do not account for one of the C$^\alpha$H protons.

Several signals were shifted upfield in the 0 to −20 ppm chemical shift region. Hyperfine-shifted signals that exhibit a small downfield chemical shift or even an upfield shift are typical of protons on ligands associated with an Fe(II) center of an antiferromagnetically coupled Fe(III)/Fe(II) [2Fe-2S] cluster (*22*). Signals L (−11.4 ppm) and M (−15.5 ppm) disappear in D_2O solution, with the disappearance of signal M occurring over a period of several days at room temperature. These two protons can be definitively assigned to the two histidine N$^{\epsilon 2}$H protons. The remaining signals were tentatively assigned to the four C$^\beta$H and two C$^\alpha$H protons of the coordinated histidine ligands on the basis of their chemical shifts and T_1 values. However, two of these resonances could be due to the histidine C$^{\epsilon 1}$H or C$^{\delta 2}$H protons since both histidine ligands are bound in an N-δ fashion as shown by ENDOR (*14*) and X-ray crystallographic studies (*25*) of related Rieske-type centers.

The 400 MHz ^{1}H NMR spectrum of the oxidized Rieske-type protein in MOPS-buffered H_2O solution, pH 7.2, at 300 K is shown in Figure 1B. Two hyperfine-shifted signals were observed in the 40−10 ppm chemical shift range. Signal A is likely the four C$^\beta$H protons of the two cysteine ligands bound to the [2Fe-2S] cluster, while signal B is probably at least one of the C$^\alpha$H cysteine protons. Both of these signals exhibit a Curie-type temperature dependence that is typical of strongly antiferromagnetically coupled [2Fe-2S] clusters. Strong antiferromagnetic coupling does not provide an effective pathway for electronic relaxation; thus, relatively broad hyperfine-shifted ^{1}H NMR resonances are observed. However, strong magnetic coupling provides a less paramagnetic sample so the chemical shift is smaller than would be observed in the absence of magnetic coupling. This spectrum is similar to those observed for several other [2Fe-2S] ferredoxins after oxidation (*21*, *22*).

nOe Difference Spectra of the Rieske-Type Protein from Xanthobacter Strain Py2. Definitive assignment of each of the observed hyperfine-shifted signals for the Rieske-type protein from *Xanthobacter* strain Py2 were obtained from nuclear Overhauser effect (nOe) saturation transfer experiments. For paramagnetic metalloproteins with favorably short electronic relaxation times, steady-state nOe has been shown to be a useful tool for identifying pairs of nuclei in close proximity to each other (*17*, *21*, *22*). For the reduced [2Fe-2S] cluster, nOe difference spectra were obtained for signals A and B at 300 K (Figure 2). Irradiation of signal A for 10 ms showed clear nOe cross-relaxation to signal B. Likewise, when B was irradiated for 10 ms, a clear nOe connection was observed to signal A. In order to verify that irradiation of B for 10 ms did not in turn partially irradiate signal A, which is 9 ppm away, the decoupler was calibrated by irradiating a single resonance of ferricytochrome *c* that was less than 2 ppm away from a second resonance (*26*). In this experiment, irradiation of either signal showed no

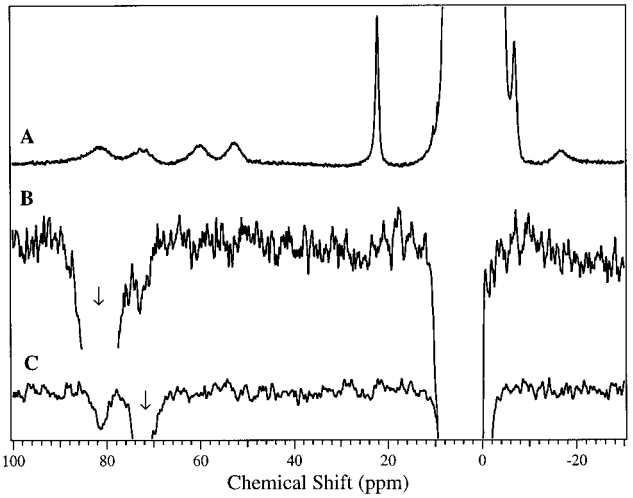

FIGURE 2: nOe difference ^{1}H NMR spectra of a 1 mM sample of [2Fe-2S]$^{1-}$ (reduced) in D_2O at 300 K with the on-resonance decoupler pulse set at the frequency indicated by the arrow. (A) ^{1}H NMR spectrum of a 1 mM sample of [2Fe-2S]$^{1-}$ (reduced) in D_2O at 300 K in 100 mM MOPS buffer and 200 mM NaCl, pH 7.0. (B) nOe difference spectrum with the decoupler pulse centered at 82 ppm. (C) nOe difference spectrum with the decoupler pulse centered at 73 ppm.

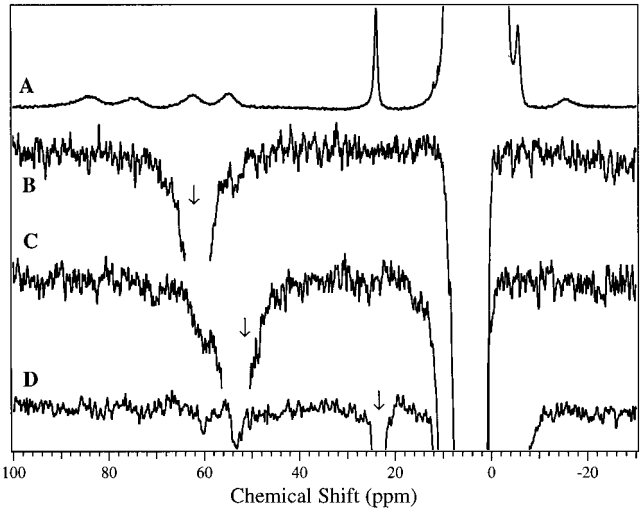

FIGURE 3: nOe difference ^{1}H NMR spectra of a 1 mM sample of [2Fe-2S]$^{1-}$ (reduced) in D_2O at 300 K with the on-resonance decoupler pulse set at the frequency indicated by the arrow. (A) ^{1}H NMR spectrum of a 1 mM sample of [2Fe-2S]$^{1-}$ (reduced) in D_2O at 300 K in 100 mM MOPS buffer and 200 mM NaCl, pH 7.0. (B) nOe difference spectrum with the decoupler pulse centered at 62 ppm. (C) nOe difference spectrum with the decoupler pulse centered at 54 ppm. (D) nOe difference spectrum with the decoupler pulse centered at 24 ppm.

irradiation of the second. These data indicate that, under our pulsing conditions, decoupler power spillover did not occur for signals greater than or equal to 2 ppm away. Therefore, protons A and B are in close proximity to one another and make up a C$^\beta$H pair from a cysteinyl ligand. The corresponding C$^\alpha$H proton of the cysteinyl ligand was not observed and likely has a Larmor frequency within the diamagnetic envelope.

nOe difference spectra were also recorded for signals C, D, and E at 300 K (Figure 3). When signal C was irradiated for 10 ms, clear nOe cross-relaxation was observed to signal D. Likewise, irradiation of signal D showed clear nOe cross-

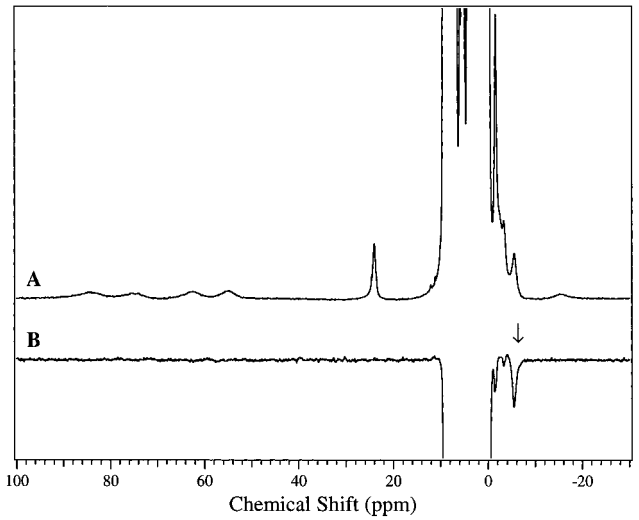

FIGURE 4: nOe difference ^{1}H NMR spectra of a 1 mM sample of $[2Fe\text{-}2S]^{1-}$ (reduced) in D_2O at 300 K with the on-resonance decoupler pulse set at the frequency indicated by the arrow. (A) ^{1}H NMR spectrum of a 1 mM sample of $[2Fe\text{-}2S]^{1-}$ (reduced) in D_2O at 300 K in 100 mM MOPS buffer and 200 mM NaCl, pH 7.0. (B) nOe difference spectrum with the decoupler pulse centered at −5.4 ppm.

relaxation to signal C. Irradiation of signal E for 10 ms showed clear nOe cross-relaxation to signals C and D. These data confirm that the protons making up signals C and D are in close proximity to one another and are also in close proximity to the proton making up signal E. This type of nOe pattern is indicative of an ABX spin system. Therefore, protons C and D make up a C$^\beta$H pair from the second cysteinyl ligand, while E is the corresponding C$^\alpha$H proton of the cysteinyl ligand. Assignment of the remaining upfield-shifted signals are difficult due to their short T_1 values and poor dispersion. The only signal that was resolved enough for one-dimensional nOe difference spectroscopy was signal K. Therefore, an nOe difference spectrum was recorded for signal K at 300 K (Figure 4). Irradiation of signal K with a mixing time of 10 ms showed clear nOe cross-relaxation to signals J and H. Again, an nOe pattern of this type is indicative of an ABX spin system. Since the two histidine ligands coordinated to the Fe(II) center are N-δ bound, proton K is likely the histidine C$^\beta$H proton while J and H are the second C$^\beta$H and C$^\alpha$H protons, respectively, from the same histidine ligand. The remaining signals F and G are assigned, by default, to the C$^\beta$H proton pair from the same histidine ligand, while the corresponding C$^\alpha$H proton is assigned to signal I.

Temperature Studies. The temperature dependence of the hyperfine-shifted signals over the temperature range 276−308 K observed for the Rieske-type protein from *Xanthobacter* strain Py2 are shown as Curie plots in Figure 5. Both Curie and pseudo-Curie temperature dependencies were observed for sets of hyperfine-shifted protons. Signals A−E followed Curie-like behavior (contact shift decreases with increasing temperature), while signals F−K and M exhibit pseudo-Curie behavior (contact shift increases with increasing temperature). These data indicate that the Fe(III/II) ions are moderately antiferromagnetically coupled (*21*, *22*). At no temperature examined (276−308 K) could the second C$^\alpha$H cysteinyl proton be observed. These data further support the conclusion that signals A−E are due to C$^\beta$H and C$^\alpha$H cysteinyl ligand protons and that signals F−K and M

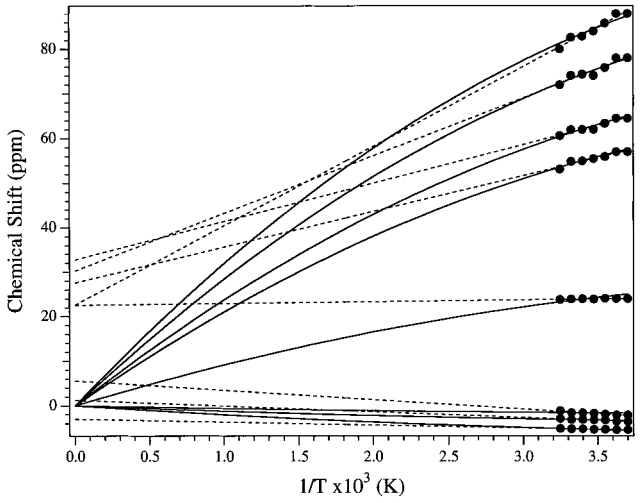

FIGURE 5: Temperature dependence of the hyperfine-shifted ^{1}H NMR resonances of a 1 mM sample of $[2Fe\text{-}2S]^{1-}$ (reduced) in D_2O between 276 and 308 K. The dashed lines are linear least-squares fits to the data, while the solid lines are fits to eq 4.

result from histidine ligand protons.

Inspection of Figure 5 reveals that the temperature dependence of the hyperfine-shifted signals for the Rieske-type ferredoxin from *Xanthobacter* strain Py2 does not strictly follow Curie behavior. Deviations of the hyperfine shift from Curie law can be understood by considering the presence of two closely spaced energy levels where the difference between the ground and excited states are on the order of *k*T. Since the reduced Rieske-type ferredoxin [2Fe-2S] cluster contains two high-spin iron centers that are antiferromagnetically coupled (*27*−*31*), a term is added to the spin Hamiltonian of the form $-2JS_1S_2$, where S_1 and S_2 are the spin vectors of the high-spin Fe(III) and Fe(II) ions, respectively, and J is the exchange coupling constant. The states of a spin-coupled system of this type can be described by the total spin S where $S = {}^1/_2$, ${}^3/_2$, ${}^5/_2$, ${}^7/_2$, and ${}^9/_2$ (*32*). Therefore, the energies relative to the ground state are 0, $-3J$, $-8J$, $-15J$, and $-24J$. At low temperatures ($kT \ll 3J$), only the ground ($S = {}^1/_2$) state will be significantly populated; however, the first excited state will become populated as the temperature is raised ($kT \approx 3J$).

In a very elegant study by Shokhirev and Walker (*33*), the temperature dependence of hyperfine-shifted signals for multilevel systems were described. Their approach takes into account the thermal population of the excited state, which allowed accurate simulation of the temperature dependence of the hyperfine-shifted signals for several low-spin Fe(III) model hemes and heme proteins (*34*, *35*). By averaging the equations describing the hyperfine shift with their Boltzman weighting factors, the observed chemical shift (δ_n) is given by

$$\delta_n = (1/Z) \sum \delta_{n,\mathrm{L}} W_\mathrm{L} \exp^{-E_\mathrm{L}/kT} \qquad (2)$$

where $\delta_{n,\mathrm{L}}$ is the hyperfine shift of nucleus n in a pure electronic state L, Z is the statistical sum

$$Z = \sum W_\mathrm{L} \exp^{-E_\mathrm{L}/kT} \qquad (3)$$

and W_L is the statistical weight of state L ($W_\mathrm{L} = 2S_\mathrm{L} + 1$). For a two-level case, such as that found for the Rieske-type ferredoxin from *Xanthobacter* strain Py2 where only the *S*

Chart 1

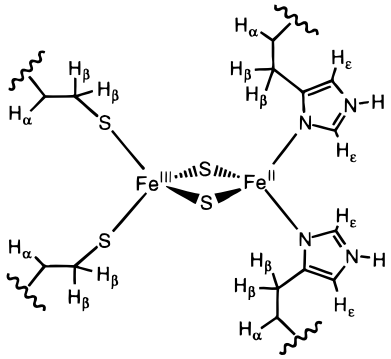

$= {}^1/_2$ and ${}^3/_2$ levels will be significantly populated at room temperature (*32*), eqs 2 and 3 can be combined and reduced to

$$\delta_n = \frac{1}{T}\frac{W_1F_{n,1} + W_2F_{n,2}\exp^{-\Delta E_L/T}}{W_1 + W_2\exp^{-\Delta E_L/T}} \qquad (4)$$

where $F_{n,1}$ and $F_{n,2}$ are the Curie factors of the ground and excited states, respectively, and $\Delta E_L = (E_2 - E_1)$. The temperature data obtained for eight of the observed hyperfine-shifted signals for the Rieske-type [2Fe-2S] ferredoxin from *Xanthobacter* strain Py2 were fit to eq 4 (Figure 5) using the program TDF21LVL kindly provided by Nikolai Shokhirev and Ann Walker (*33*). These fits provided a ΔE_L value of 185 ± 39 cm^{-1}, which gives a $-2J$ value of 124 ± 26 cm^{-1}, consistent with the two iron centers being moderately antiferromagnetically coupled (*32*).

DISCUSSION

Combination of the reported spectroscopic data, which includes electronic absorption, circular dichroism, EPR, ENDOR, Mössbauer, and resonance Raman spectroscopy indicates that Rieske-type [2Fe-2S] clusters, in all cases, contain two cysteine and two histidine ligands (*13*, *14*, *36*−*38*). This unusual ferredoxin ligand sphere provides distinct spectroscopic signatures from ferredoxins that contain an all cysteine ligand sphere. For example, Rieske-type [2Fe-2S] clusters exhibit characteristic EPR signals having $g_{ave} \sim 1.91$ ($g_1 = 2.01$; $g_2 = 1.92$; $g_3 = 1.76$) compared to $g_{av} \sim 1.96$ for ferredoxins, red-shifted electronic absorption spectra with decreased molar absorptivities, and distinct circular dichroism spectra. In addition, Rieske-type [2Fe-2S] clusters have reduction potentials that fall in the range $+350$ to -150 mV, whereas ferredoxins are typically much lower, near -400 mV. These data have lead to the conclusion that reduced Rieske-type [2Fe-2S] clusters contain a high-spin Fe(III) ion antiferromagnetically coupled to a high-spin Fe(II) ion, providing a total spin of ${}^1/_2$. It was also concluded that the two iron ions were bridged by two inorganic sulfur atoms and that the Fe(III) ion was ligated by two cysteinyl ligands while the Fe(II) ion was coordinated by two histidine groups (Chart 1). Recently, this structure was confirmed by X-ray crystallographic studies on the Rieske-type [2Fe-2S] cluster from the bovine heart mitochondrial cytochrome bc_1 complex (*25*).

The Rieske-type ferredoxin described herein is an electron transfer component of the alkene monooxygenase multienzyme complex from *Xanthobacter* strain Py2. The ferredoxin mediates electron transfer between a reductase component, which provides the reductant for O_2 activation and reduction, and an oxygenase component, which contains the catalytic center for alkene epoxidation, as illustrated in Scheme 1. The Rieske-type ferredoxin from *Xanthobacter* strain Py2 was previously shown to have a molecular weight of 13 300 by mass spectrometry and 26 000 by gel-filtration chromatography, indicating a homodimeric structure (*13*). Immunoblot analysis of cell-free extracts of *Xanthobacter* Py2 revealed that the Rieske-type ferredoxin accumulated during cell growth with propylene as a carbon source but was absent from cells grown with glucose or acetone as the sole carbon sources. Electronic absorption, EPR, and circular dichroism spectra of the oxidized and dithionite-reduced [2Fe-2S] cluster revealed the presence of a single [2Fe-2S] Rieske-type center in each protein monomer (*13*). The reduction potential of this Rieske-type [2Fe-2S] cluster was shown to be -49 mV (*13*).

The reduced Rieske-type ferredoxin from *Xanthobacter* strain Py2 exhibits several well-resolved hyperfine-shifted ^{1}H NMR resonances in the 90 to -20 ppm chemical shift range arising from ligand protons of the [2Fe-2S] cluster. Upon oxidation, only two broad resonances are observed, which indicates that the two Fe(III) ions are strongly antiferromagnetically coupled. Similar spectra have been reported for [2Fe-2S]-containing ferredoxins from algae, plants, bacteria, and vertebrates (*21*). The observation of both downfield and upfield hyperfine-shifted signals for the reduced Rieske-type [2Fe-2S] cluster reflects the ligation to Fe(III) and Fe(II) centers, respectively (*22*). Protons associated with ligands bound to an Fe(III) center ($S = {}^5/_2$) antiferromagnetically coupled to an Fe(II) center ($S = 2$) will feel a negative spin orientation (aligned with the external magnetic field) causing the contact hyperfine shift to be downfield. On the other hand, protons on ligands bound to the Fe(II) ion will sense a positive spin orientation (opposed to the magnetic field) and will be contact-shifted in the upfield direction (*32*). Therefore, protons associated with the Fe(III) and Fe(II) centers can be quickly differentiated solely on the basis of their chemical shift.

By comparison with ^{1}H NMR data reported for conventional [2Fe-2S] ferredoxins, the downfield-shifted signals were initially assigned to C$^\beta$H and C$^\alpha$H protons of the cluster cysteinyl ligands. All of the observed signals had T_1 values less than 4 ms and line widths typically greater than 400 Hz. These properties render signal assignment by 2D methods impossible at this time; therefore, one-dimensional steady-state nOe methods were used with a mixing time of 10 ms. The use of longer mixing times allowed spin diffusion to occur, which provided unreliable nOe difference spectra. The nOe data revealed that signals A and B are closely associated with one another and thus make up a C$^\beta$H cysteine pair of protons. Likewise, signals C and D were assigned to a second C$^\beta$H cysteine pair of protons and signal E was assigned to the C$^\alpha$H proton. The assignment of E to the C$^\alpha$H proton is clear, based on nOe cross-relaxation, a longer T_1 value than signals C and D, and a smaller chemical shift and line width compared to signals C and D. The second C$^\alpha$H proton cysteinyl proton corresponding to the first C$^\beta$H cysteine pair of protons was not observed. Since the hyperfine shifts of protons of this type are strongly influenced by the angle between the C$^\beta$H and C$^\alpha$H protons, this C$^\alpha$H proton does not likely exhibit a large hyperfine

Scheme 1

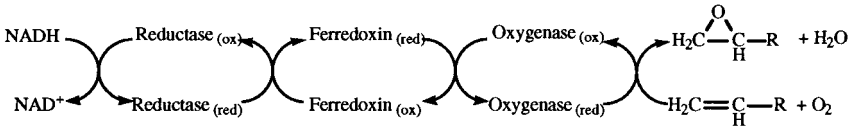

shift and is therefore buried under the diamagnetic envelope.

The nOe intensities shown in Figures 2 and 3 are not a quantitative measure of the percent nOe since all spectra have been baseline-subtracted to alleviate a sigmodal baseline role typical of spectra recorded under conditions of large sweep widths and fast repetition rates. Even so, the observed nOes are still larger than one might predict theoretically ($\eta = \sigma_{ij}T_1$). Two reasons exist for the observed added intensity. First, the enzyme sample was 1 mM in protein so it was 2 mM in iron−sulfur cluster. Concentrated enzyme samples are significantly more viscous, altering the protein tumbling time, which enhances the observed nOes. Second, the fact that the Rieske-type protein from *Xanthobacter* strain Py2 is a dimer of 13 kDa. subunits suggests that under the experimental conditions (1 mM protein) higher oligomeric structures might exist that would also significantly alter the protein tumbling time and, consequently, the intensity of the observed nOes. For example, if the Rieske-type protein from *Xanthobacter* strain Py2 tumbled like an 80 kDa. enzyme due to viscosity and oligomerization, an nOe between 40% and 60% would be expected for geminal proton pairs.

Eight signals are observed in the 0 to −20 ppm chemical shift region that can be initially assigned to protons associated with coordinated histidine residues. Exchange of H_2O with D_2O buffered solution reveals that two signals are solvent exchangeable. These two solvent-exchangeable signals are assigned to the two histidine $N^{\epsilon 2}H$ protons of coordinated histidine residues bound to the Fe(II) center of the Rieske-type [2Fe-2S] cluster. Signal L exchanges very rapidly upon exchange into D_2O buffer; however, signal M exchanges very slowly over 24 h and a partial signal can still be observed even after 2 weeks in D_2O buffer. Therefore, signal L is likely hydrogen-bound to another side chain that markedly inhibits its exchange rate. Definitive assignment of the remaining signals in the 0 to −10 ppm chemical shift range is difficult because of the very short T_1 values (all <4 ms). One-dimensional steady-state nOe methods could be used to assign signal K since its Larmor frequency was sufficiently different from its nearest neighbors so decoupler spillover did not occur. Irradiation of K with a mixing time of 10 ms revealed that K is associated with signals J and H. These three signals are assigned to the $C^{\beta}H$ and $C^{\alpha}H$ protons of a coordinated histidine residue. By default, signals I, F, and E can be assigned to the $C^{\beta}H$ and $C^{\alpha}H$ protons of the second coordinated histidine residue.

Complete assignment of the observed hyperfine-shifted ^{1}H NMR resonances, coupled with the temperature dependence of the hyperfine-shifted resonances, allows information regarding the magnetic properties of the reduced [2Fe-2S] cluster to be obtained. Signals A−E follow Curie behavior (contact shift decreases with increasing temperature), while signals F−K and M follow pseudo-Curie behavior. The observed ^{1}H NMR spectrum of the reduced Rieske [2Fe-2S] cluster is similar to reduced vertebrate ferredoxins, which also have more positive reduction potentials (*39*, *40*). Reduced vertebrate ferredoxins also exhibit both upfield and downfield hyperfine-shifted signals, all of which display Curie or pseudo-Curie type behavior. For mixed-valent Fe(III/II) dinuclear centers, the stronger the spin-coupling between the two metal ions, the larger the upfield shift for those protons associated with the Fe(II) center (*32*). Therefore, the reduced Rieske [2Fe-2S] cluster from *Xanthobacter* strain Py2 contains an antiferromagnetically coupled Fe(III/II) pair that falls into the moderate spin-coupling regime.

Fits of the temperature data for each observed resonance provides a ΔE_L value of 185 ± 26 cm^{-1}, which gives a $-2J$ value of 124 ± 26 cm^{-1}. This value is consistent with the two iron centers in the [2Fe-2S] Rieske-type center being moderately antiferromagnetically spin-coupled. Only a single magnetic study has been reported for a Rieske-type ferredoxin [2Fe-2S] cluster. In this study, that temperature dependence of the observed EPR signal was used to estimate a $-2J$ value of 130 cm^{-1}. Therefore, the $-2J$ value obtained in this study is nearly identical to that obtained from EPR data. While the error associated with the $-2J$ value obtained from the temperature dependence of the ^{1}H NMR signals is large due to the relatively small temperature range available for studies of this kind, the NMR data clearly provide a reasonable estimate for the magnetic properties of the spin-coupled [2Fe-2S] clusters. In addition, the temperature dependence of the observed hyperfine-shifted resonances, along with their complete assignment, verifies that both histidine ligands are bound to the Fe(II) center and that both cysteinyl moieties are coordinated to the Fe(III) center.

Combination of the NMR data presented herein with the recent X-ray crystallographic data for the Rieske-type ferredoxin from the bovine heart mitochondrial cytochrome bc_1 complex provides insight into the potential electron transfer pathway utilized by Rieske-type centers (*25*). Examination of the X-ray structure reveals a (μ-sulfido)-diiron core with two cysteine ligands (Cys139 and Cys158) bound to one iron center and two histidine ligands (His141 and His161) bound to the second iron center. Each iron resides in a distorted tetrahedral coordination geometry. As shown by X-ray crystallography and supported by the NMR data presented herein, as well as previous ENDOR and Mössbauer data, the Fe(II) center is bound by two histidine ligands in an N-δ fashion (*14*, *38*). The crystallographic data also revealed that the [2Fe-2S] cluster is located on the surface of the protein with the Fe(II) ion, bound by two histidine ligands, closer to the surface of the protein than the Fe(III) center. Having the Fe(II) center near the surface of the protein is consistent with the single-electron oxidation of the Fe(II) ion following electron transfer. The fact that signal M exhibits a slow H/D exchange rate suggests that one histidine residue of the Rieske cluster found in *Xanthobacter* strain Py2 is more solvent-exposed then the second. Therefore, the more solvent-exposed histidine residue is likely the group that makes up the electron transfer pathway from the Fe(II) center.

In summary, the present work represents the first complete assignment of hyperfine-shifted ^{1}H NMR signals observed

from a Rieske-type [2Fe-2S] cluster. These data confirm that two histidine residues are bound to the Fe(II) center while two cysteine residues are coordinated to the Fe(III) center. Moreover, these data confirm that the alkene oxidizing system found in *Xanthobacter* strain Py2 contains a Rieske-type electron transfer component (*13*). These data provide a fingerprint of Rieske-type protein [2Fe-2S] clusters that will be useful in the future characterization of complex formation between components of this alkene oxidizing system.

ACKNOWLEDGMENT

We thank Dr. Nilolai Shokhirev and Professor Ann Walker, from the University of Arizona, for providing us with the temperature dependence curve-fitting program TDF2LVL. We also wish to thank Dr. Brian Bennett and Mr. Jeff Allen for helpful discussions.

REFERENCES

1. Anemüller, S., Schmidt, C. L., Schäfer, G., and Teixeira, M. (1993) *FEBS Lett. 318*, 61−64.
2. Byrne, A. M., Kukor, J. J., and Olsen, R. H. (1995) *Gene 154*, 65−70.
3. Fee, J. A., Findling, K. L., Yoshida, T., Hille, R., Tarr, G. E., Hearshen, D. O., Dunham, W. R., Day, E. P., Kent, T. A., and Münck, E. (1984) *J. Biol. Chem. 259*, 124−133.
4. Iwasaki, T., Isogai, Y., Iizuka, T., and Oshima, T. (1995) *J. Bacteriol. 177*, 2576−2582.
5. Link, T. A., Hatzfeld, O. M., Unalkat, P., Shergill, J. K., Cammack, R., and Mason, J. R. (1996) *Biochemistry 35*, 7546−7552.
6. Pikus, J. D., Studts, J. M., Achim, C., Kauffmann, K. E., Münck, E., Steffan, R. J., McClay, K., and Fox, B. G. (1996) *Biochemistry 35*, 9106−9119.
7. Rosche, B., Fetzner, S., Lingens, F., Nitschke, W., and Riedel, A. (1995) *Biochim. Biophys. Acta: Protein Struct. Mol. Enzymol. 1252*, 177−179.
8. Geary, P. J., Saboowalla, F., Patil, D., and Cammack, R. (1984) *Biochem. J. 217*, 667−673.
9. Haddock, J. D., and Gibson, D. T. (1995) *J. Bacteriol. 177*, 5834−5839.
10. Haigler, B. E., and Gibson, D. T. (1990) *J. Bacteriol. 172*, 465−468.
11. Subramanian, V., Liu, T.-N., Yeh, W.-K., Serdar, C. M., Wackett, L. P., and Gibson, D. T. (1985) *J. Biol. Chem. 260*, 2355−2363.
12. Romanov, V., and Hausinger, R. P. (1994) *J. Bacteriol. 176*, 3368−3374.
13. Small, F. J., and Ensign, S. A. (1997) *J. Biol. Chem. 272*, 24913−24920.
14. Gurbiel, R., Batie, C. J., Sivaraja, M., True, A. E., Fee, J. A., Hoffman, B. M., and Ballou, D. P. (1989) *Biochemistry 28*, 4861−4871.
15. Lippard, S. J., and Berg, J. M. (1994) *Principles of Bioinorganic Chemistry*, pp 302−311, University Science Books, Mill Valley, CA.
16. Batie, C. J., LaHaie, E., and Ballou, D. P. (1987) *J. Biol. Chem. 262*, 1510−1518.
17. La Mar, G. N., and de Ropp, J. S., Eds. (1993) *NMR Methodology for Paramagnetic Proteins*, Vol. 12, pp 1−78, New York.
18. Bertini, I., and Luchinat, C. (1986) *NMR of Paramagnetic Molecules in Biological Systems*, Benjamen & Cummings, Menlo Park, CA.
19. Bertini, I., Molinari, N., and Niccolai, N. (1991) *NMR and Biomolecular Structure*, VCH, New York.
20. Bertini, I., and Luchinat, C. (1992) in *Physical Methods for Chemists* (Drago, R. S., Eds.) pp 500−556, Harcourt Brace Jovanovich, Orlando, FL.
21. Bertini, I., Turano, P., and Vila, A. J. (1993) *Chem. Rev. 93*, 2833−2932.
22. Cheng, H., and Markley, J. L. (1995) *Annu. Rev. Biophys. Biomol. Struct. 24*, 209−237.
23. Markley, J. L., Xia, B., Chae, Y. K., Cheng, H., Westler, W. M., Pikus, J. D., and Fox, B. G. (1995) in *Protein Structure Function Relationships* (Zaidi, Z., and Smith, D., Eds.) Plenum Press, London (in press).
24. Kerby, R., and Zeikus, J. G. (1987) *J. Bacteriol. 169*, 5605−5609.
25. Iwata, S., Saynovits, M., Link, T. A., and Michel, H. (1997) manuscript in preparation.
26. Lanzilotta, W. N., Holz, R. C., and Seefledt, L. C. (1995) *Biochemistry 34*, 15646−15653.
27. Salerno, J. C., Ohnishi, T., Blum, H., and Leigh, J. S. (1977) *Biochim. Biophys. Acta 494*, 191−197.
28. Gayda, J. P., Gibson, J. F., Cammack, R., Hall, D. O., and Mullinger, R. (1976) *Biochim. Biophys. Acta 434*, 154−163.
29. Bertrand, P., and Gayda, J. P. (1979) *Biochim. Biophys. Acta 579*, 107−121.
30. Bertrand, P., Gayda, J. P., Fee, J. A., Kuila, D., and Cammack, R. (1987) *Biochim. Biophys. Acta 916*, 24−28.
31. Petersson, L., Cammack, R., and Rao, K. K. (1980) *Biochim. Biophys. Acta 622*, 18−24.
32. Banci, L., Bertini, I., and Luchinat, C. (1990) *Struct. Bond. 72*, 113−136.
33. Shokhirev, N. V., and Walker, F. A. (1995) *J. Phys. Chem. 99*, 17795−17804.
34. Horrocks, W. D., and Greenberg, E. S. (1973) *Biochim. Biophys. Acta 322*, 38−44.
35. Horrocks, W. D., and Greenberg, E. S. (1974) *Mol. Phys. 27*, 993−999.
36. Stephens, P., J., Thomson, A. J., Dunn, J. B. R., Keiderling, T. A., Rawlings, J., Rao, K. K., and Hall, D. O. (1978) *Biochemistry 17*, 4770−4778.
37. Verhagen, M. F. J. M., Link, T. A., and Hagen, W. R. (1995) *FEBS Lett. 361*, 75−78.
38. Fee, J. A., Findling, K. L., Yoshida, T., Hille, R., Tarr, G. E., Hearshen, D. O., Dunham, W. R., Day, E. P., Kent, T. A., and Münck, E. (1984) *J. Biol. Chem. 259*, 124−133.
39. Skjeldal, L., Markley, J. L., Coghlan, V. M., and Vickery, L. E. (1991) *Biochemistry 30*, 9078.
40. Miura, R., and Ichikawa, Y. (1991) *J. Biol. Chem. 266*, 6252.

BI971831T